

LETTER • OPEN ACCESS

## To what extent can cirrus cloud seeding counteract global warming?

To cite this article: Blaž Gasparini *et al* 2020 *Environ. Res. Lett.* **15** 054002

View the [article online](#) for updates and enhancements.



## LETTER

## To what extent can cirrus cloud seeding counteract global warming?

## OPEN ACCESS

## RECEIVED

29 November 2019

## REVISED

15 January 2020

## ACCEPTED FOR PUBLICATION


30 January 2020

## PUBLISHED

23 April 2020

Original content from this work may be used under the terms of the [Creative Commons Attribution 4.0 licence](#).

Any further distribution of this work must maintain attribution to the author(s) and the title of the work, journal citation and DOI.

Blaž Gasparini<sup>1,3,4</sup> , Zachary McGraw<sup>2</sup>, Trude Storelvmo<sup>2</sup> and Ulrike Lohmann<sup>1</sup><sup>1</sup> ETH Zürich, Zürich, Switzerland<sup>2</sup> University of Oslo, Oslo, Norway<sup>3</sup> now at University of Washington, United States of America.<sup>4</sup> Author to whom any correspondence should be addressed.E-mail: [blazg@uw.edu](mailto:blazg@uw.edu)**Keywords:** geoengineering, cirrus clouds, cirrus cloud seeding, cirrus cloud thinning, climate damage, precipitation extremes, climate modelingSupplementary material for this article is available [online](#)**Abstract**

The idea of modifying cirrus clouds to directly counteract greenhouse gas warming has gained momentum in recent years, despite disputes over its physical feasibility. Previous studies that analyzed modifications of cirrus clouds by seeding of ice nucleating particles showed large uncertainties in both cloud and surface climate responses, ranging from no effect or even a small warming to a globally averaged cooling of about 2.5 °C. We use two general circulation models that showed very different responses in previous studies, ECHAM6-HAM and CESM-CAM5, to determine which radiative and climatic responses to cirrus cloud seeding in a 1.5 × CO<sub>2</sub> world are common and which are not. Seeding reduces the net cirrus radiative effect for  $-1.8 \text{ W m}^{-2}$  in CESM compared with only  $-0.8 \text{ W m}^{-2}$  in ECHAM. Accordingly, the surface temperature decrease is larger in CESM, counteracting about 70% of the global mean temperature increase due to CO<sub>2</sub> and only 30% in ECHAM. While seeding impacts on mean precipitation were addressed in past studies, we are the first to analyze extreme precipitation responses to cirrus seeding. Seeding decreases the frequency of the most extreme precipitation globally. However, the extreme precipitation events occur more frequently in the Sahel and Central America, following the mean precipitation increase due to a northward shift of the Intertropical Convergence Zone. In addition, we use a quadratic climate damage metric to evaluate the amount of CO<sub>2</sub>-induced damage cirrus seeding can counteract. Seeding decreases the damage by about 50% in ECHAM, and by 85% in CESM over the 21 selected land regions. Climate damage due to CO<sub>2</sub> increase is significantly reduced as a result of seeding in all of the considered land regions.

**1. Introduction**

The Paris agreement, signed by the United Nations member states in 2015, aims to limit the anthropogenically driven global warming to well below 2 °C warming with respect to preindustrial levels. Despite the agreement, the gap between current anthropogenic greenhouse gas emission pathways and the 2 °C climate goal continues to increase (IEA 2019). Therefore, the time window to achieve the Paris goal by only pursuing a rapid energy system transformation in combination with negative emissions is rapidly closing (Rogelj *et al* 2015). Moreover, the emission scenarios compatible with Paris Agreement goals largely rely on

extensive use of biomass energy with carbon capture and storage (Sanderson *et al* 2016), which was found to be too ambitious (Vaughan and Gough 2016).

Yet, current political negotiations have not considered the deployment of some form of solar radiation management (SRM) to help achieving the Paris Agreement targets. Keith and MacMartin (2015) argue that an SRM scenario which would offset only half of the anthropogenic climate forcing can maximize the benefits better than ones targeting a full recovery of surface temperature, due to less dramatic changes in hydrological cycle or ozone loss. A study by Tilmes *et al* (2016) assessed the impact of a temporary application of stratospheric sulfur injections in a delayed

climate mitigation scenario. They assumed an RCP8.5 emission scenario pathway until the year 2040, when the Earth has warmed by about 2 °C, after which the emissions follow a decarbonisation pathway with emissions peaking in 2050 and becoming negative in year 2100. Following their emission scenario, stratospheric sulfur injections have to last for as long as 160 years, to limit some of the negative impacts of climate change, in particular the occurrence of hot temperature extremes.

Numerous studies showed that any form of SRM significantly perturbs the climate system due to differences between longwave (LW) CO<sub>2</sub> forcing and incoming shortwave (SW) radiative effects leading to changes in the surface energy budget and precipitation (Bala *et al* 2008, Robock *et al* 2008, Boucher *et al* 2013, Kravitz *et al* 2014). A new geoengineering method has been suggested recently, targeting mainly LW radiation to better counteract the climatic impacts of a CO<sub>2</sub> increase. Cirrus cloud seeding, first proposed by Mitchell and Finnegan (2009), acts primarily on LW radiation. Cirrus clouds generally form at altitudes between 5 and 18 km at temperatures below the homogeneous freezing temperature of water (approximately −38 °C) and are therefore composed of ice crystals only. They have a net warming effect on climate as they reflect only little solar radiation while they significantly modulate the LW radiation fluxes. A decrease in cirrus cloud frequency obtained by seeding with solid aerosols would therefore lead to larger outgoing LW radiation and a surface cooling (Lohmann and Gasparini 2017).

The mechanism relies on the competition between homogeneous nucleation and solid aerosol (also known as ice nucleating particles, INPs) mediated heterogeneous freezing in cirrus clouds. When cirrus form by homogeneous freezing of solution droplets (Ickes *et al* 2015), this leads to the formation of a large number of small ice crystals. The introduction of a well defined number concentration of effective INPs changes the microphysical properties of cirrus clouds (Kärcher and Lohmann 2003, Storelvmo *et al* 2013). Ice crystals then form by deposition nucleation on the surface of INPs, allowing nucleation to occur at lower updraft velocities or higher temperatures. This decreases the ambient relative humidity with respect to ice (RH<sub>ice</sub>) and prevents further homogeneous nucleation events leading to a small number concentration of larger ice crystals, which sediment faster, shorten the cirrus lifetime, and make the cirrus clouds more transparent for radiation (Lohmann and Gasparini 2017).

Studies using simulations of increased ice crystal sedimentation velocity, which serve as an analog of cirrus cloud seeding with INPs, show that its fast, temperature independent response leads to an enhancement of the atmospheric water cycle (Kristjánsson *et al* 2015, Jackson *et al* 2016). Idealized seeding leads to enhanced atmospheric cooling, and an increase in latent heat fluxes and precipitation. Seeding therefore avoids the

weakening of the hydrological cycle, thus counteracting the effect of CO<sub>2</sub> in a better way than SRM-based geoengineering studies. However, its impact on the precipitation extremes has not yet been studied.

The main aim of this study is to evaluate robust and uncertain climate responses to cirrus seeding in the ECHAM6-HAM and CESM-CAM5 general circulation models (GCMs) (also named ECHAM and CESM in most of the text for brevity), which have been shown previously to respond differently to the addition of artificial INPs. The study builds upon known micro- and macrophysical changes in cirrus seeded with INPs in the two GCMs and focuses on the impacts of cirrus seeding on temperature and precipitation.

## 2. Methods

### 2.1. Model and simulation setup

We use the ECHAM6 GCM (Stevens *et al* 2013) coupled with the HAM2 aerosol module (Zhang *et al* 2012, Neubauer *et al* 2014). The model has a resolution of 1.875° × 1.875° with 31 vertical layers extending to 30 km altitude. ECHAM6-HAM uses a two moment cloud scheme (Lohmann *et al* 2007) with a cirrus microphysical scheme, which allows competition between homogeneous and heterogeneous nucleation and the deposition of water vapor on pre-existing ice crystals (Kärcher *et al* 2006, Kuebbeler *et al* 2014, Gasparini and Lohmann 2016). Convection is parameterized by the mass-flux scheme of Tiedtke (1989) with modifications for deep convection from Nordeng (1994). The model has been previously evaluated with satellite observations (Gasparini *et al* 2018) and was used in several process-based studies that focused on cirrus clouds and their responses to various forcings (Kuebbeler *et al* 2012, 2014, Gasparini and Lohmann 2016, Gasparini *et al* 2017). ECHAM6-HAM is run in the mixed layer ocean setup, which explicitly simulates the interactions between the atmosphere and the surface layer of the ocean and sea ice, but neglects possible responses of deep ocean currents.

We also use the NCAR Community Earth System Model (CESM) version 1.2.2, which couples separate model components for the atmosphere, ocean, land, and sea ice (Hurrell *et al* 2013). We use the atmospheric component Community Atmosphere Model (CAM) version 5.3, run at a horizontal resolution of 1.9° latitude by 2.5° longitude with 30 vertical levels. The standard configuration for CAM uses the Zhang-McFarlane deep convection scheme (Zhang and McFarlane 1995), with the dilute plume closure assumption by Neale *et al* (2008). The shallow convection parameterization follows Park and Bretherton (2009). The stratiform cloud scheme is handled by two separate components: a macrophysics scheme for grid-scale condensation and cloud fraction calculations (Park *et al* 2014) and a microphysics

**Table 1.** Simulation terminology and their respective properties.

Simulation	CO <sub>2</sub> concentration	seed
REF	353.9 ppm	/
1.5CO <sub>2</sub>	530.9 ppm	/
SEED	530.9 ppm	1 INP l <sup>-1</sup> at night only (ECHAM) 18 INPs l <sup>-1</sup> (CESM)

parameterization for sub-grid scale cloud processes (Morrison and Gettelman 2008). However, for ice nucleation in cirrus clouds, the parameterization scheme by Barahona and Nenes (2009) was used. The default ice cloud macrophysics scheme in CAM 5.3 is the modified Slingo (1987) scheme as in Gettelman *et al* (2008). The aerosol size distribution is described by a 3-mode scheme described in Liu *et al* (2012). The atmosphere is coupled to a Slab Ocean Model (SOM) to include the thermodynamic effects of the ocean mixed-layer. Its spatially varying depth is based on observations of the annual-mean mixed-layer depth (Kiehl *et al* 2006). The SOM treats the ocean as motionless and perfectly mixed throughout its depth.

We perform three simulations with each model (table 1): a reference simulation with present day CO<sub>2</sub> concentrations (REF), a simulation with 1.5 × present day CO<sub>2</sub> concentrations (1.5CO<sub>2</sub>), and a cirrus geoengineering simulations for the 1.5 × CO<sub>2</sub> climate. The simulations are run for 80 years (ECHAM) or 100 years (CESM), where we always consider only the last 60 years of data with a monthly averaged output frequency. The CESM simulation is longer due to a longer equilibration time compared to ECHAM. The seeding strategy in ECHAM follows the results of Gasparini *et al* (2017): all cirrus clouds (clouds at temperatures colder than −35 °C) are seeded with a concentration of 1 INP l<sup>-1</sup> using 50 μm large seeding nuclei only during night. Such setup does not only decrease the amount of seeded material needed but was also shown to increase the cooling efficacy and decrease the convective precipitation responses (Gasparini *et al* 2017).

The CESM seeding strategy assumes a globally uniform seeding of 18 INP l<sup>-1</sup> using 10 μm large seeding nuclei as in the HOMHET\_50% scenario in Storerlmo and Herger (2014). CESM1 (unlike CESM2) does not consider pre-existing ice crystals, primarily because their existence has not been documented. The differences in simulation of cirrus clouds and their responses to seeding aerosol lead to a different choice of seeding strategies between the two models. A CESM-like seeding strategy would in ECHAM lead to overseeding and a warming of climate, while seeding with only 1 INP l<sup>-1</sup> in CESM would lead only to a minimal climatic cooling effect. We note that the total mass of delivered particles is due to the cubic dependence of mass on seeding aerosol radius about 3.5 times larger in the ECHAM seeding scenario compared to

the CESM one. We stress that the main purpose of this study is not to understand the subtle differences in microphysical modeling setups and underlying microphysical responses but to rather evaluate the climatic responses of the modeled maximal cirrus seeding effects in both models.

As the atmospheric models are coupled to a shallow mixed-layer ocean, it takes approximately 20 (ECHAM) to 40 (CESM) years to come into climatic equilibrium. Thus we use only data from the last 60 simulated years. The CO<sub>2</sub> concentrations for the reference (present day) conditions are taken as 353.9 ppm (1990 concentrations, Taylor *et al* 2012), while the CO<sub>2</sub> concentrations in the 1.5 × CO<sub>2</sub> simulations are 530.9 ppm, roughly equivalent to the concentrations in the last decades of the 21st century from the RCP4.5 scenario (van Vuuren *et al* 2011). Therefore, we can compare our increased emission simulation result to CMIP5 model output for years 2081–2100 (Collins *et al* 2013). We use the double sided Student's t-test at the 95% significance level to test the robustness of our results.

## 2.2. Damage function

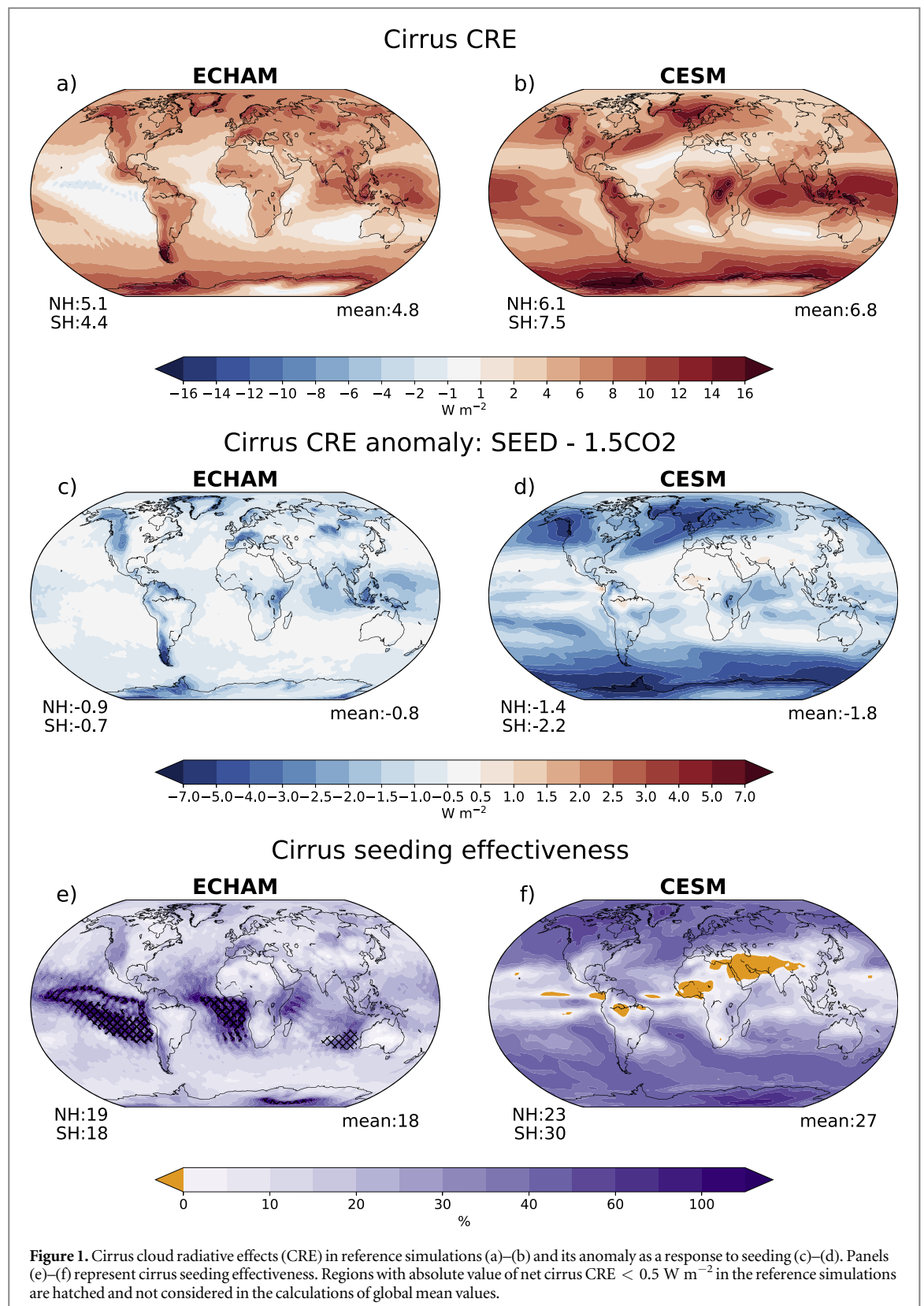
We define a damage function with a quadratic dependence on mean temperature and precipitation anomalies normalised by their respective natural variability (one standard deviation range of the present day climate simulation) as

$$\text{Damage} = \left( \frac{\Delta T}{T_{stdev}} \right)^2 + \left( \frac{\Delta p}{p_{stdev}} \right)^2. \quad (1)$$

Studies assessing climate change impacts frequently use quadratic damage functions (Keller *et al* 2004, Nordhaus 2008, Weitzman 2010, Nordhaus and Sztorc 2013, Kravitz *et al* 2014) or some higher order functional form (Goes *et al* 2011). However, the precise functional shape does not considerably affect the outcomes of our moderate climate change scenario, when temperatures do not exceed 2 °C of warming with respect to the reference simulation (Weitzman 2010, Kopp *et al* 2012).

The function is nondimensional, and defined as strictly positive (or equal to zero), where a higher value means a larger damage with respect to the present day climate. We use an arbitrary scale with no upper limit. The calculated damage serves thus only as a tool to compare the 1.5CO<sub>2</sub> simulation with the geoengineered simulations.

To make our damage function more relevant for the society, we consider only land gridboxes, which are divided into 21 larger geographical units (Giorgi and Francisco 2000), covering all continents except Antarctica (table S2). The damage function input values are area weighted means of temperature and precipitation, separately shown in figures S4 and S5 are available at [stacks.iop.org/ERL/15/054002/mmedia](https://stacks.iop.org/ERL/15/054002/mmedia).



### 3. Results

#### 3.1. Cirrus cloud radiative effects and radiative responses to seeding

We define cirrus clouds as all clouds at temperatures colder than  $-35 \text{ }^\circ\text{C}$  and compare the cloud radiative effect (CRE) of all clouds formed at such conditions

(figures 1(a) and (b)). In both models the cirrus CRE peaks in the tropics, particularly in the convectively active Warm Pool region, and in the storm track regions. CESM simulates a higher ice water content at cirrus levels (figure S1), resulting in a more positive net CRE ( $6.8 \text{ W m}^{-2}$ ) compared with ECHAM ( $4.8 \text{ W m}^{-2}$ ). Nevertheless, the radiative effects of both



models lie within the range of the available satellite observations of cirrus CRE (Hong *et al* 2016, Matus and L'Ecuyer 2017).

The larger, more positive cirrus CRE alone, implies a larger radiative impact of seeding in CESM than in ECHAM, assuming the same effectiveness of seeding strategies, which can be seen in figures 1(c), (d). However, as shown by panels e and f, the models do not only differ in the simulated unperturbed cirrus and their CRE, but also in the seeding effectiveness, defined as  $-100 * \frac{\text{cirrusCREanomaly}}{\text{cirrusCRE}}$ . A higher effectiveness points out at a better cancellation of the (positive) cirrus CRE by seeding. The seeding effectiveness is larger in most regions in CESM compared to ECHAM, with globally averaged values of 27% and 18%, respectively. In CESM a large fraction of extratropical cirrus are dominated by homogeneous freezing and are therefore sensitive to the introduction of seeding aerosol. Seeding aerosol decrease cirrus cloud frequency and optical properties, leading to a globally averaged net CRE anomaly of  $-1.8 \text{ W m}^{-2}$  (figure 1(d)). In contrast, only a small fraction of cirrus simulated by the ECHAM model forms by homogeneous freezing (Gasparini and Lohmann 2016), limiting the overall seeding effectiveness and the net seeding effect to  $-0.8 \text{ W m}^{-2}$  in the global average (figure 1(c)). Interestingly, the seeding in ECHAM is most effective over mountains and in parts of the tropics. The seeding effectiveness in ECHAM is slightly larger in the NH, while CESM has a 7% larger effectiveness in the SH. The CESM model simulates a smaller dust burden in the SH and consequently a higher proportion of homogeneously formed cirrus clouds (Storelmo and Herger 2014). On the other hand, negative effectiveness implies a more positive cirrus CRE due to cirrus seeding, known as 'overseeding' (Storelmo and Herger 2014). Overseeding occurs particularly in areas dominated by heterogeneous cirrus cloud formation mechanisms, such as the Middle East and Northern Africa in CESM (figure 1(f)), or Australia in ECHAM (figure 1(e)). In summary, a larger reference (unperturbed) cirrus CRE and a higher seeding effectiveness due to more homogeneously formed cirrus clouds lead to a more than two times larger radiative response to seeding in CESM compared to ECHAM ( $-1.8$  versus  $-0.8 \text{ W m}^{-2}$ ).

### 3.2. Climatic responses

#### 3.2.1. Mean temperature responses

The  $1.5 \times \text{CO}_2$  concentrations in ECHAM cause a global average warming of  $1.8 \text{ }^\circ\text{C}$  (figure 2(a)), which falls in the middle of the likely range of the end-of-the-century warming by the IPCC models that follow the RCP4.5 emission scenario. CESM on the other hand has a higher climate sensitivity (Tan *et al* 2016) which results in a  $2.0 \text{ }^\circ\text{C}$  global warming (figure 2(d)). The mean temperature responses to a combination of increased  $\text{CO}_2$  concentration and seeding of cirrus

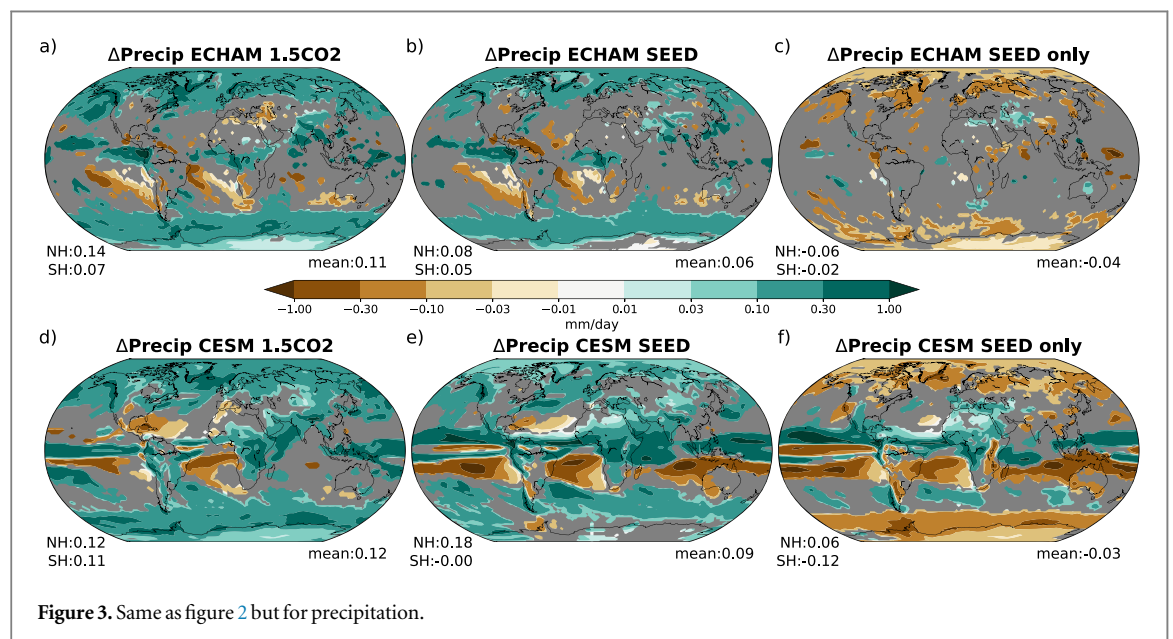
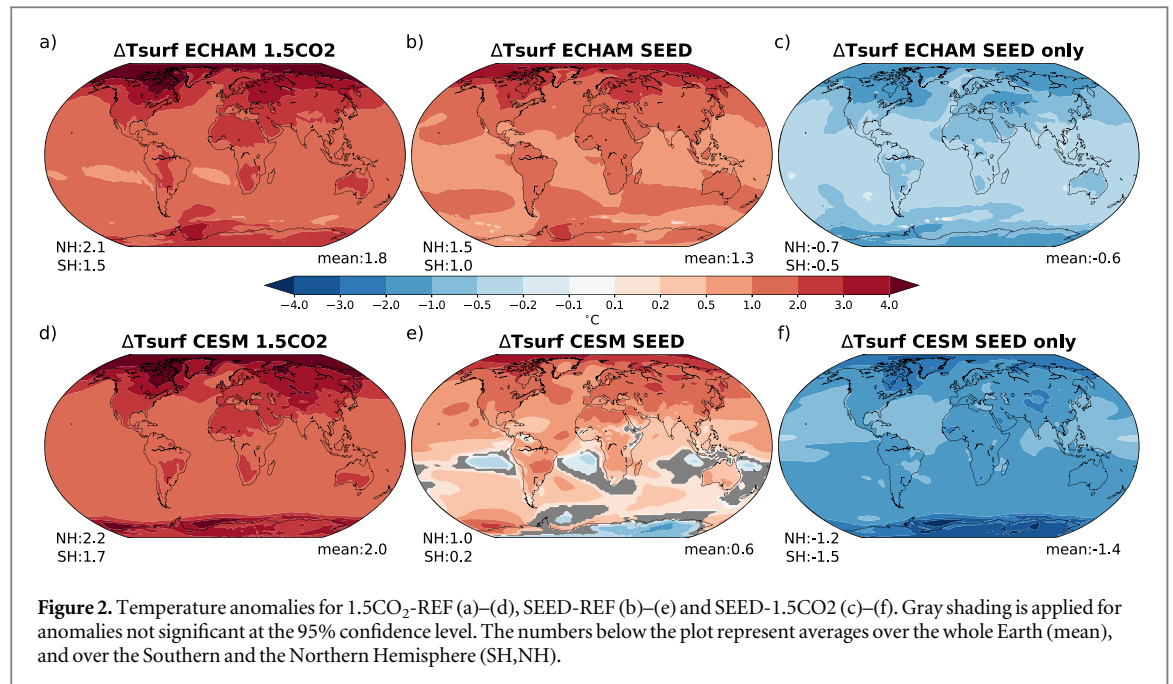
clouds differ substantially between the two models (figures 2(b) and (e)). In ECHAM seeding counteracts about  $0.6 \text{ }^\circ\text{C}$  of the global mean temperature increase due to the  $\text{CO}_2$ , resulting in a net global temperature increase of  $1.3 \text{ }^\circ\text{C}$  with respect to present day conditions. Seeding is more effective in CESM, counteracting about  $1.4 \text{ }^\circ\text{C}$  of the global mean temperature increase due to  $\text{CO}_2$ , leading to a warming of only  $0.6 \text{ }^\circ\text{C}$ .

Temperature responses to seeding are tightly connected to CRE anomalies resulting from seeding (figure 1) described in the previous subsection. The temperature response is always stronger in the winter hemisphere, where the scattering of SW radiation by cirrus is minimal due to low insolation. Interestingly, the effect of seeding in CESM is larger in the Southern Hemisphere (SH) than in the Northern Hemisphere (NH, figure 2(f)), while ECHAM shows the opposite response (figure 2(c)). SH high latitude cirrus form almost exclusively by homogeneous ice nucleation in CESM (Storelmo and Herger 2014), while ECHAM preferentially forms homogeneous cirrus over mountains, which are more frequent in the NH compared with the SH (Gasparini and Lohmann 2016).

#### 3.2.2. Mean precipitation responses

The globally averaged precipitation increase of 3.5% (ECHAM) and 3.8% (CESM) in the  $1.5\text{CO}_2$  climate is mainly driven by the slow, surface temperature dependent response to the  $\text{CO}_2$  concentration increase. The rise in surface temperature increases the amount of water vapor in the atmosphere, enhances its radiative cooling and increases precipitation (Bala *et al* 2010, Bony *et al* 2013, Pendergrass and Hartmann 2014). Precipitation in both models increases mainly in the tropics and high latitudes, while many subtropical regions experience a drying (figures 3(a), (d) and 4(a), (d)), consistent with studies of precipitation responses to  $\text{CO}_2$  forcing (Chou and Neelin 2004, Held and Soden 2006).

SEED alone cannot compensate for the  $\text{CO}_2$  driven precipitation responses—however, the global average precipitation increase is about 40% weaker in ECHAM and 20% weaker in CESM compared to the respective  $1.5\text{CO}_2$  simulations (figures 3(b) and (e)). Seeding has in absolute terms a smaller impact on precipitation in ECHAM compared to CESM. Interestingly, the Intertropical Convergence Zone (ITCZ) in the CESM SEED simulation shifts northwards compared to both REF and  $1.5\text{CO}_2$  simulations (figures 3(e), (f) and 5(b)), leading to a drier South America and Maritime Continent, and at the same time increasing precipitation in the Sahel and Central America. The driver of the shift is the temperature imbalance between the two hemispheres (figure 2(f)), which pushes the ITCZ towards the warmer hemisphere, as shown in previous work on anthropogenic and volcanic aerosol emissions (Rotstajn and Lohmann 2002, Haywood *et al* 2013). The drying of



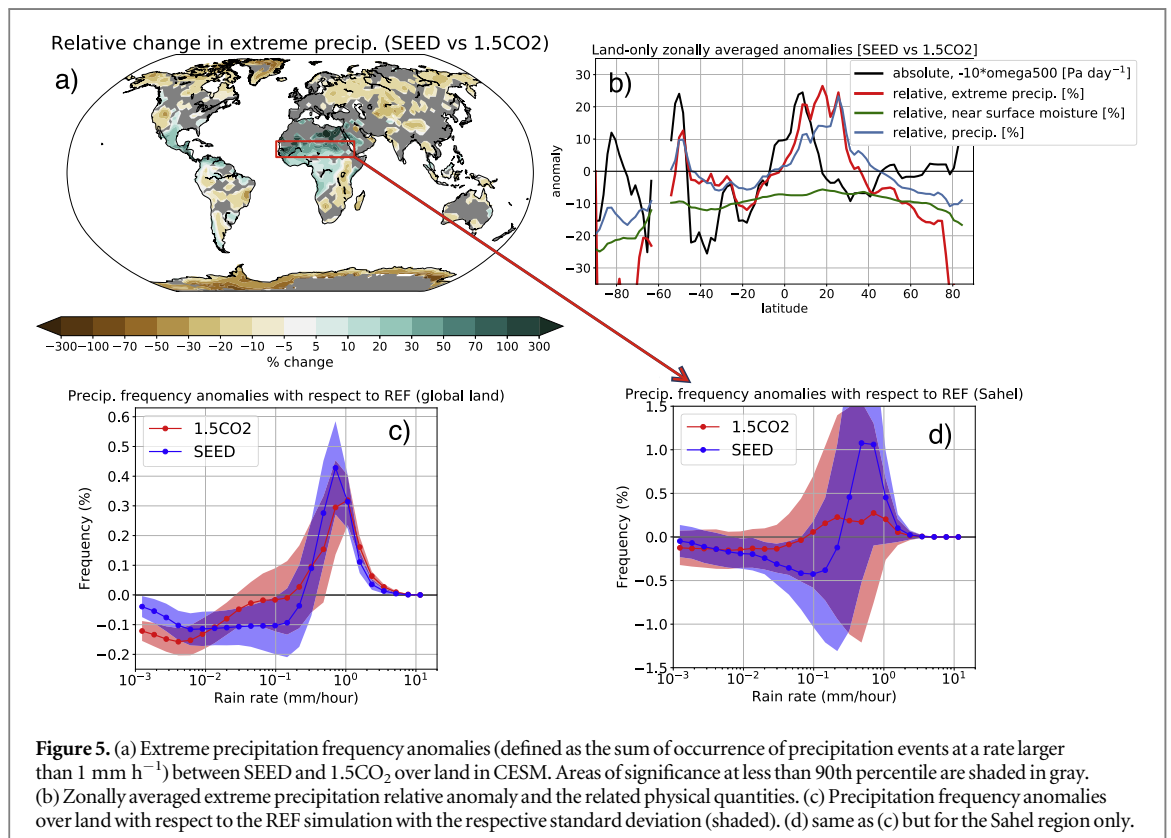
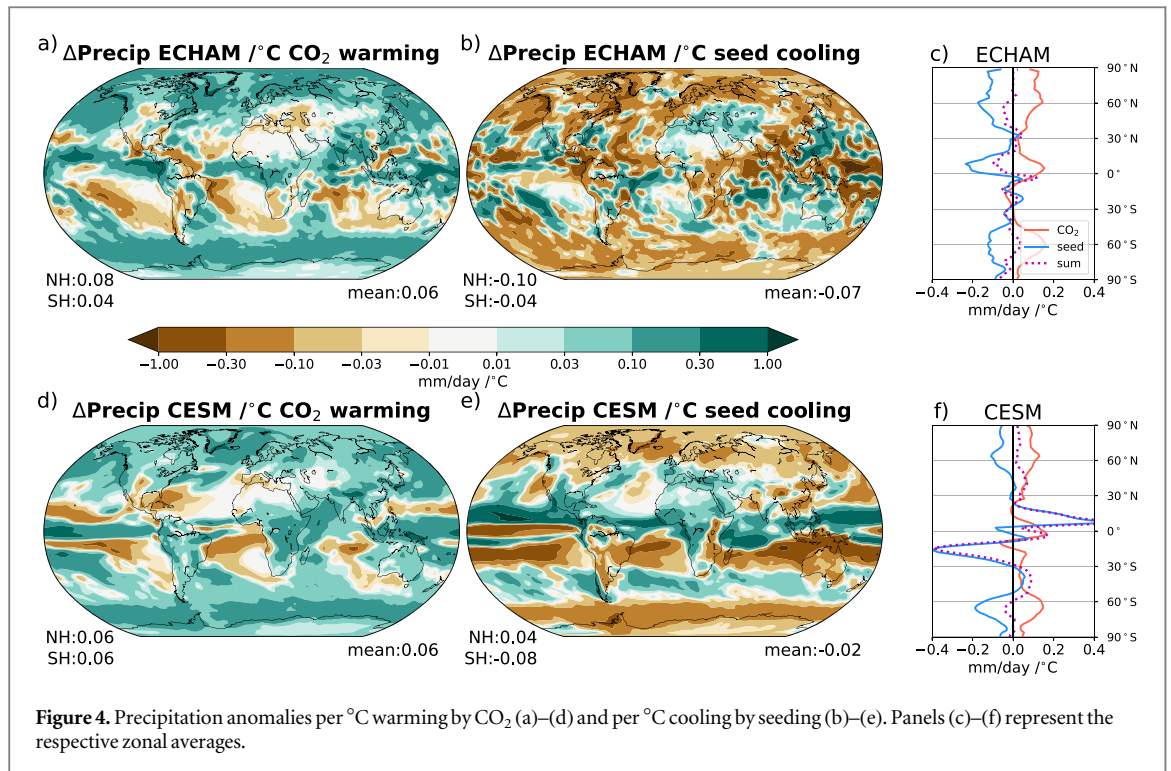
the SH subtropics in CESM is centered over oceans, limiting its potential impact on agriculture and society. ECHAM, on the other hand, does not simulate significant hemispheric precipitation shifts, as its radiative and temperature responses between the two hemispheres are more balanced (figures 2(b) and (c)).

We additionally compare normalized hydrological responses of both models to a unit of warming by CO<sub>2</sub> (figures 4(a) and (d)) and cooling by cirrus seeding (figures 4(b) and (e)). The sign of the precipitation anomalies and their regional pattern for both models changes when comparing the warming with the cooling case. Precipitation responses to seeding in ECHAM are of similar magnitude but opposite sign compared to the CO<sub>2</sub> warming case. Interestingly, in CESM seeding leads to one third the change in globally

averaged precipitation compared to the CO<sub>2</sub> warming simulation, which may be caused by either the direct microphysical enhancement of precipitation due to seeding or an increased convective activity due to seeding. The zonally averaged extratropical precipitation anomalies in CESM are, on the other hand, similar for the warming and cooling case (figure 4(f)). In the tropics, however, the signal is dominated by the northward ITCZ shift.

### 3.2.3. Precipitation extremes

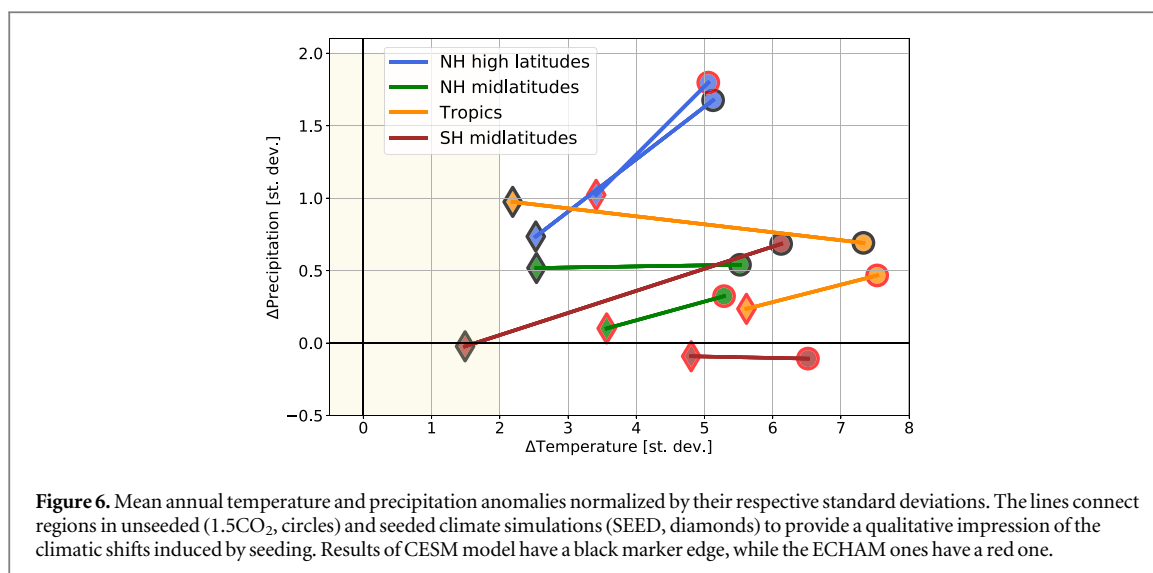
Seeding perturbations rapidly change cirrus cloud properties, potentially leading to a direct microphysical perturbation of precipitation. Moreover, a decreased occurrence of cirrus clouds leads to a decreased upper tropospheric relative humidity and temperatures.



The resulting increased upper tropospheric radiative cooling implies a precipitation increase (Pendergrass and Hartmann 2014), as observed in previous cirrus seeding studies (Storelvmo and Herger 2014, Gasparini *et al* 2017). However, as seeding cools surface temperature, moisture decreases, decreasing both the mean and

the extreme precipitation (O’Gorman and Schneider 2009). It is therefore interesting to look at how extreme precipitation events respond to seeding in a 1.5 × CO<sub>2</sub> climate. We define all precipitation events with precipitation rates larger than 1 mm h<sup>-1</sup> as extreme precipitation, sampled at every model timestep. We sort





the precipitation events in 29 predefined bins between 0.001 and 100 mm h<sup>-1</sup>. Figure 5(a) shows relative changes in the frequency of high precipitation events over land between SEED and 1.5CO<sub>2</sub> simulations for CESM model (defined as  $\frac{100 \cdot (\text{SEED} - 1.5\text{CO}_2)}{1.5\text{CO}_2}$ ), isolating the seeding signal. In the global average, the frequency of extreme precipitation decreases, particularly over the SH and areas north of 35°N, as expected due to the decreased atmospheric moisture content (figure 5(b)). The SEED simulation shares a lot of the signal with the 1.5CO<sub>2</sub> simulation, which leads to a shift of precipitation distribution to higher rates (figure 5(c)). Interestingly, the effect of seeding alone leads to a narrowing of the precipitation distribution, decreasing the frequency of high precipitation events compared to 1.5CO<sub>2</sub>, and increasing the frequency of moderate precipitation events. The distributions shifts due to seeding result from the interplay between the temperature-mediated decrease in the intensity of the hydrological cycle on one hand, and an increased convective precipitation frequency due to enhanced atmospheric cooling on the other hand (figure S2).

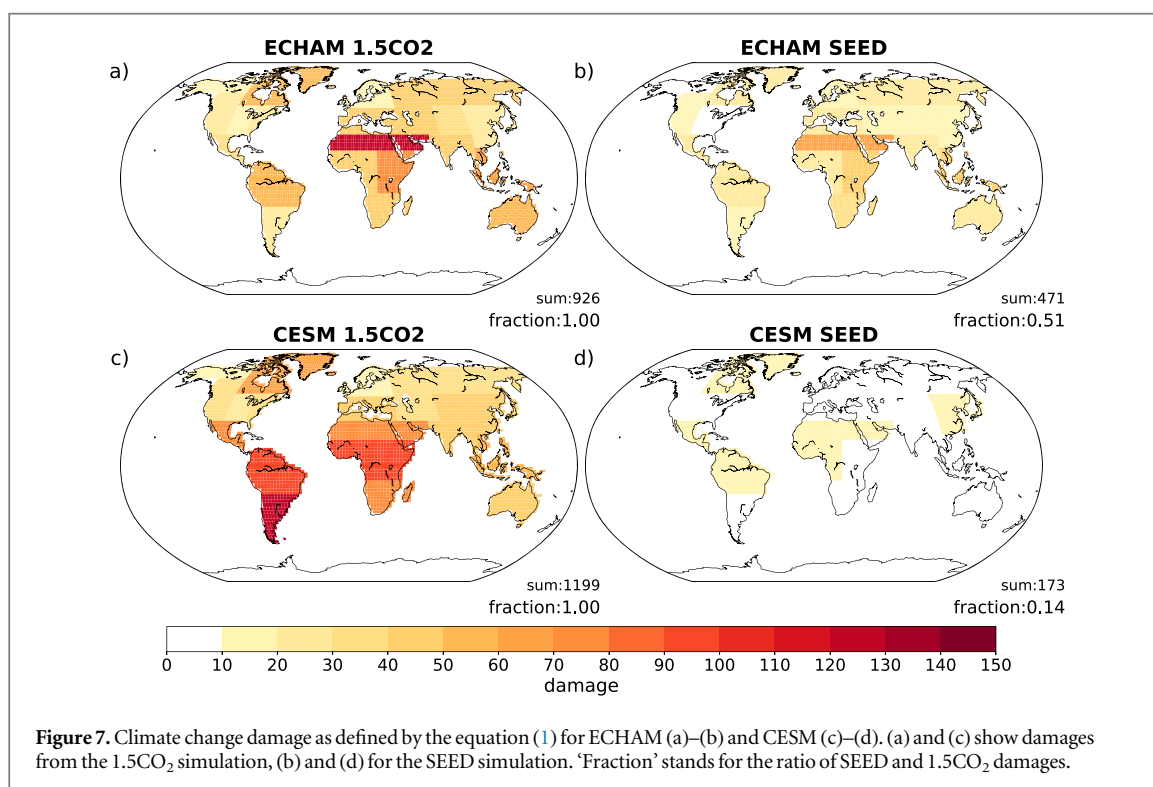
The precipitation extremes significantly increase over central and Northern Africa and parts of the Middle East, Central America, and northernmost South America. This increase is connected to the northward shift of the ITCZ (figure 3(f)), and the associated increases in updraft velocities and mean precipitation (figure 5(b)). Figure 5(d) shows changes in the precipitation distribution for the Sahel region (10°–20° N, 20°W–40°E), in which seeding increases precipitation rates for precipitation rates of about 1 mm h<sup>-1</sup> by up to 1%. However, at the extreme tail of the distribution, for precipitation rates beyond 2 mm h<sup>-1</sup>, the frequency of precipitation is similar or even slightly higher in the 1.5CO<sub>2</sub> simulation. We speculate that this is a response to lower moisture availability in the colder SEED simulation. Changes in moisture content were shown to be the dominant driving mechanisms of extreme

precipitation events, increasing its relative importance the higher the precipitation intensity (O’Gorman and Schneider 2009, Sugiyama *et al* 2010).

The frequency of both convective and large-scale precipitation extremes increases after an instantaneous seeding perturbation, when the surface temperatures did not yet have time to adjust to the resulting radiative imbalance (figure S2, years 1–2 of the simulation). The origin of this increase could be related both to a direct microphysical perturbation or to a rapid adjustment to seeding leading to increased atmospheric cooling. The two sources of rapid precipitation changes cannot be separated by the current set of simulations. Consistently with figure 5(c), the global land precipitation extremes in SEED show a decrease for model years 40–100 compared to REF, following a surface temperatures cooling of 1.4 °C.

#### 3.2.4. Normalized temperature and precipitation responses

Figure 6 shows a perspective on the relative size of the annual mean precipitation and temperature anomalies for the land regions in 4 selected latitudinal bands. Temperature experiences a large positive shift of about 5–7 standard deviations with increased CO<sub>2</sub> concentrations. Interestingly, the normalized temperature responses to both CO<sub>2</sub> and seeding do not show a polar amplification pattern due to the large temperature variability in the high latitudes compared with the tropics. This is consistent with studies on the time emergence of climate signals which first detect a significant climate change signal in low latitude regions (Mahlstein *et al* 2011, Hawkins and Sutton 2012). The precipitation changes are less pronounced and more uneven: NH high latitudes are most sensitive to both CO<sub>2</sub> and seeding forcing with increases of about 1.5 standard deviations in the 1.5CO<sub>2</sub> simulation, compared with changes smaller than 1 standard deviation in other regions. The NH high latitudes also respond to seeding with the largest



precipitation decreases of about 1 (CESM) or 0.5 (ECHAM) standard deviations. Interestingly, the seeding in CESM leads to a small increase in precipitation over tropical land, differently from responses of other regions to seeding. This is related to the northward shift of the ITCZ (figure 3(e)) and the tropical land mass distribution, where a larger fraction of tropical land lies north of the ITCZ. Those regions experience a significant wetting that is driving the increase in mean tropical precipitation. CESM SEED simulation brings both temperature and precipitation in the selected latitudinal bands close to the range of  $\pm 2$  standard deviations from the present day climate, only within a small distance in temperature space from the mean climate goal (shaded area in figure 6). In ECHAM SEED simulation the temperature deviations in these land regions remain noticeably outside the mean climate goal.

### 3.3. Damage avoided

In order to better evaluate the avoided warming and precipitation increase by increased CO<sub>2</sub> and by cirrus geoengineering, we assess the damages with respect to the present day REF climate simulation with the help of the quadratic damage function for the 21 global land regions (Giorgi and Francisco 2000) similarly to what Kravitz *et al* (2014) did for the SRM case. The annual mean damages are the largest in the 1.5CO<sub>2</sub> simulation (figure 7). Most of the damage is related to changes in temperature: the regional precipitation anomalies are small and fall within the natural variability, while the surface temperature signal often emerges out of the natural variability range (figures S4 and S5). The

damage by increased CO<sub>2</sub> concentrations is largest in the Sahara, East Africa, and parts of South East Asia for ECHAM. The damage is about 30% larger in the CESM model due to its stronger temperature and precipitation response to the CO<sub>2</sub> forcing. The most affected regions are Equatorial Africa, South and Central America.

SEED offsets about 50% of the annual average damage compared with the 1.5CO<sub>2</sub> simulation in the ECHAM model. The damage pattern remains similar as in 1.5CO<sub>2</sub>, with Africa being most affected by changes in climate. However, as the seeding is most effective in high latitudes, the regions of Greenland, Northern Asia, and Alaska are subject to considerably smaller damage compared with the 1.5CO<sub>2</sub> simulation. Seeding in the CESM model on the other hand decreases climate damage to small values, showing only residual temperature-related damage in several tropical regions, as well as in northern North America and Greenland.

## 4. Discussion and conclusions

We used a series of simulations of climate models coupled to the surface ocean layer to evaluate the responses to a cirrus seeding geoengineering strategy. We injected efficient ice nucleating particles using the climatically most effective known modeling strategy in each of the two climate models used. The ECHAM and CESM GCMs differ significantly in the modeled cirrus clouds, their formation mechanisms, radiative effects, and finally, also their responses to seeding (figures 1 and S1, Storelvmo and Herger 2014, Gasparini and

Lohmann 2016, Gasparini *et al* 2017). Nevertheless, the study shows several common climatic responses to seeding in a high CO<sub>2</sub> climate:

- Cirrus seeding in both models leads to a temperature and precipitation decrease.
- The precipitation decrease is a result of the slow, temperature mediated, slowdown of the water cycle. Contrary, both models have previously shown small precipitation increases to fast responses to seeding (e.g. Storelvmo and Herger 2014, Gasparini *et al* 2017).
- Both models roughly agree on the precipitation responses at the annual and regional level with CESM showing a significantly larger hydrological sensitivity compared to ECHAM both with respect to seeding and CO<sub>2</sub> perturbations.
- Climate damage due to a CO<sub>2</sub> increase is significantly reduced as a result of seeding in all of the considered land regions. In other words, there is no region, which would experience a higher degree of damage when seeding is applied compared with the CO<sub>2</sub> increase only. Cirrus seeding therefore decreases the level of global disparity caused by climate change, which affects some regions more than others.

Only a few studies have so far addressed the changes in climate extremes in geoengineering experiments (Tilmes *et al* 2013, Curry *et al* 2014, Aswathy *et al* 2015), while none of them analyzed responses to cirrus cloud seeding. Our study represents a first attempt to study changes in precipitation extremes in cirrus seeding simulations. Seeding was shown to reduce the frequency of occurrence of high precipitation events at the global level in CESM model. Nevertheless, some NH subtropical regions experienced increases of occurrence of all but the most extreme rain rates. However, as our data is limited to results of the CESM GCM only, results have to be taken with caution. The analysis of mechanisms driving precipitation extreme changes due to cirrus seeding has to be addressed in future work with multimodel studies, including other socially socially relevant metrics, for instance changes in agricultural productivity (Xia *et al* 2014).

While the results of our seeding simulations are consistent with previously published literature (Muri *et al* 2014, Storelvmo *et al* 2014, Kristjánsson *et al* 2015, Jackson *et al* 2016, Gasparini *et al* 2017, Gruber *et al* 2019), care has to be taken when evaluating the magnitude and regional patterns of the responses. Our work points out a large discrepancy in temperature response to seeding between the two models, which can be traced back to the significantly different cirrus cloud properties and formation mechanisms in the present day climate (Storelvmo and Herger 2014,

Gasparini and Lohmann 2016, Gasparini *et al* 2018). This consequently leads to a different radiative effectiveness of the simulated seeding strategies. The large changes in simulated cirrus clouds call for a coordinated modeling intercomparison study focusing on cirrus cloud micro- and macrophysical properties, formation mechanisms, lifecycle, and climatic impacts. The spread in simulated cirrus properties is not surprising, given the large uncertainties in space-based retrievals of ice water content, ice crystal radius and number (Duncan and Eriksson 2018, Sourdeval *et al* 2018) and limited *in situ* measurements at cirrus conditions, particularly at high latitudes.

Cirrus cloud seeding is one of the most recent ideas of artificially modifying the planetary energy balance to counteract the human-caused global warming. So far, it is still highly uncertain whether such a scheme could effectively decrease the temperatures at global scales. This study pointed out its uncertain climatic responses, which depend on the details on the complexity of simulated seeding method (seeding by INPs or increasing ice crystal sedimentation velocity, Gasparini *et al* 2017), the model used, the parametrization of ice nucleation in cirrus clouds (Penner *et al* 2015, Gasparini and Lohmann 2016), and the radius of the seeded INPs (Gasparini *et al* 2017, Gruber *et al* 2019). At this stage we have no knowledge of the specific properties of the seeded particles, its injection strategies, upper tropospheric diffusion and mixing or impacts on mixed-phase clouds. Moreover, the engineering side of the problem has never been addressed in the scientific literature and it may be more challenging than for example stratospheric sulfur injections. It may well be that seeding can cool the planet only in state-of-the-art, yet still imperfect, climate models.

## Acknowledgments

BG acknowledges support from the Swiss National Science Foundation Mobility Grant P2EZP2178485. ECHAM simulations were performed on the Euler ETHZ computational cluster. CESM simulations were performed on the Yale supercomputing center. The authors would like to acknowledge helpful comments by the two anonymous reviewers. Moreover, discussions with Phil Rasch, Ben Kravitz, and Marina Dütsch helped improve the manuscript.

## Data availability statement

The data that support the findings of this study are openly available at DOI: [10.5281/zenodo.3601622](https://doi.org/10.5281/zenodo.3601622).

## ORCID iDs

Blaž Gasparini  <https://orcid.org/0000-0002-7177-0155>

## References

- Aswathy V N, Boucher O, Quaas M, Niemeier U, Muri H, Mühlmenstädt J and Quaas J 2015 Climate extremes in multi-model simulations of stratospheric aerosol and marine cloud brightening climate engineering *Atmos. Chem. Phys.* **15** 9593–610
- Bala G, Caldeira K and Nemani R 2010 Fast versus slow response in climate change: implications for the global hydrological cycle *Clim. Dyn.* **35** 423–34
- Bala G, Duffy P B and Taylor K E 2008 Impact of geoengineering schemes on the global hydrological cycle *Proc. Natl Acad. Sci.* **105** 7664–9
- Barahona D and Nenes A 2009 Parameterizing the competition between homogeneous and heterogeneous freezing in cirrus cloud formation—monodisperse ice nuclei *Atmos. Chem. Phys.* **9** 369–81
- Bony S, Bellon G, Klocke D, Sherwood S, Fermepin S and Denvil S 2013 Robust direct effect of carbon dioxide on tropical circulation and regional precipitation *Nat. Geosci.* **6** 447–51
- Boucher O *et al* 2013 Clouds and aerosols *Climate Change 2013: The Physical Science Basis. Contribution of Working Group I to the Fifth Assessment Report of the Intergovernmental Panel on Climate Change* ed T F Stocker *et al* (Cambridge: Cambridge University Press) pp 571–658
- Chou C and Neelin J D 2004 Mechanisms of global warming impacts on regional tropical precipitation *J. Clim.* **17** 2688–701
- Collins M *et al* 2013 *Long-Term Climate Change: Projections, Commitments and Irreversibility* (Cambridge: Cambridge University Press) (<https://doi.org/10.1017/CBO9781107415324.024>)
- Curry C L *et al* 2014 A multi-model examination of climate extremes in an idealized geoengineering experiment *J. Geophys. Res.: Atmos.* **119** 3900–23
- Duncan D I and Eriksson P 2018 An update on global atmospheric ice estimates from satellite observations and reanalyses *Atmos. Chem. Phys.* **18** 11205–19
- Gasparini B and Lohmann U 2016 Why cirrus cloud seeding cannot substantially cool the planet *J. Geophys. Res.: Atmos.* **121** 4877–893
- Gasparini B, Meyer A, Neubauer D, Münch S and Lohmann U 2018 Cirrus cloud properties as seen by the CALIPSO satellite and ECHAM-HAM global climate model *J. Clim.* **31**
- Gasparini B, Münch S, Poncet L, Feldmann M and Lohmann U 2017 Is increasing ice crystal sedimentation velocity in geoengineering simulations a good proxy for cirrus cloud seeding? *Atmos. Chem. Phys.* **17** 4871–85
- Gottelman A, Morrison H and Ghan S J 2008 A new two-moment bulk stratiform cloud microphysics scheme in the community atmosphere model, version 3 (CAM3): II. Single-column and global results *J. Clim.* **21** 3660–79
- Giorgi F and Francisco R 2000 Uncertainties in regional climate change prediction: a regional analysis of ensemble simulations with the HADCM2 coupled AOGCM *Clim. Dyn.* **16** 169–82
- Goes M, Tuana N and Keller K 2011 The economics (or lack thereof) of aerosol geoengineering *Clim. Change* **109** 719–44
- Gruber S, Blahak U, Haenel F, Kottmeier C, Leisner T, Muskatel H, Storelmo T and Vogel B 2019 A process study on thinning of arctic winter cirrus clouds with high-resolution ICON-ART simulations *J. Geophys. Res.: Atmos.* **124** 5860–88
- Hawkins E and Sutton R 2012 Time of emergence of climate signals *Geophys. Res. Lett.* **39** 1–6
- Haywood J M, Jones A, Bellouin N and Stephenson D 2013 Asymmetric forcing from stratospheric aerosols impacts Sahelian rainfall *Nat. Clim. Change* **3** 660–5
- Held I M and Soden B J 2006 Robust responses of the hydrological cycle to global warming *J. Clim.* **19** 5686–99
- Hong Y, Liu G and Li J-L F 2016 Assessing the radiative effects of global ice clouds based on cloudsat and CALIPSO measurements *J. Clim.* **29** 7651–73
- Hurrell J W *et al* 2013 The community earth system model: a framework for collaborative research *Bull. Am. Meteorol. Soc.* **94** 1339–60
- Ickes L, Welti A, Hoose C and Lohmann U 2015 Classical nucleation theory of homogeneous freezing of water: thermodynamic and kinetic parameters *Phys. Chem. Chem. Phys.* **17** 5514–37
- IEA 2019 Global energy and CO<sub>2</sub> status report *Technical Report* (Paris: IEA) (<https://www.iea.org/publications/freepublications/publication/GECCO2017.pdf>)
- Jackson L, Crook J and Forster P 2016 An intensified hydrological cycle in the simulation of geoengineering by cirrus cloud thinning using ice crystal fall speed changes *J. Geophys. Res.: Atmos.* **121** 6822–40
- Kärcher B, Hendricks J and Lohmann U 2006 Physically based parameterization of cirrus cloud formation for use in global atmospheric models *J. Geophys. Res.* **111** D01205
- Kärcher B and Lohmann U 2003 A parameterization of cirrus cloud formation: heterogeneous freezing *J. Geophys. Res.* **108** 4402
- Keith D W and MacMartin D G 2015 A temporary, moderate and responsive scenario for solar geoengineering *Nat. Clim. Change* **5** 201–6
- Keller K, Bolker B M and Bradford D F 2004 Uncertain climate thresholds and optimal economic growth *J. Environ. Econ. Manage.* **48** 723–41
- Kiehl J T, Shields A, Hack J J and Collins W D 2006 Climate sensitivity of the community climate system model, version 4 *J. Clim.* **19** 2584–96
- Kopp R E, Golub A, Keohane N O and Onda C 2012 The influence of the specification of climate change damages on the social cost of carbon *Economics* **6** 113
- Kravitz B *et al* 2014 A multi-model assessment of regional climate disparities caused by solar geoengineering *Environ. Res. Lett.* **9** 074013
- Kristjánsson J E, Muri H and Schmidt H 2015 The hydrological cycle response to cirrus cloud thinning *Geophys. Res. Lett.* **42** 10807–15
- Kuebbeler M, Lohmann U and Feichter J 2012 Effects of stratospheric sulfate aerosol geo-engineering on cirrus clouds *Geophys. Res. Lett.* **39** L23803
- Kuebbeler M, Lohmann U, Hendricks J and Kärcher B 2014 Dust ice nuclei effects on cirrus clouds *Atmos. Chem. Phys.* **14** 3027–46
- Liu X *et al* 2012 Toward a minimal representation of aerosols in climate models: description and evaluation in the community atmosphere model CAM5 *Geosci. Model Dev.* **5** 709–39
- Lohmann U and Gasparini B 2017 A cirrus cloud climate dial? *Science* **357** 248
- Lohmann U, Stier P, Hoose C, Ferrachat S, Kloster S, Roeckner E and Zhang J 2007 Cloud microphysics and aerosol indirect effects in the global climate model ECHAM5-HAM *Atmos. Chem. Phys.* **7** 3425–46
- Mahlstein I, Knutti R, Solomon S and Portmann R W 2011 Early onset of significant local warming in low latitude countries *Environ. Res. Lett.* **6** 034009
- Matus A V and L'Ecuyer T S 2017 The role of cloud phase in Earth's radiation budget *J. Geophys. Res.: Atmos.* **122** 1–20
- Mitchell D L and Finnegan W 2009 Modification of cirrus clouds to reduce global warming *Environ. Res. Lett.* **4** 045102
- Morrison H and Gottelman A 2008 A new two-moment bulk stratiform cloud microphysics scheme in the community atmosphere model, version 3 (CAM3): I. Description and numerical tests *J. Clim.* **21** 3642–59
- Muri H, Kristjánsson J E, Storelmo T and Pfeffer M 2014 The climatic effects of modifying cirrus clouds in a climate *J. Geophys. Res.: Atmos.* **119** 4174–91
- Neale R B, Richter J H and Jochum M 2008 The impact of convection on ENSO: from a delayed oscillator to a series of events *J. Clim.* **21** 5904–24
- Neubauer D, Lohmann U, Hoose C and Frontoso M G 2014 Impact of the representation of marine stratocumulus clouds on the anthropogenic aerosol effect *Atmos. Chem. Phys.* **14** 11997–2022
- Nordeng T E 1994 Extended versions of the convective parametrization scheme at ECMWF and their impact on the mean and transient activity of the model in the tropics



- Technical Report (Reading: ECMWF) (<https://doi.org/10.21957/e34xwhyw>)
- Nordhaus W 2008 *A Question of Balance: Weighing the Options on Global Warming Policies* (New Haven, CT: Yale University Press) pp 166–7
- Nordhaus W and Sztorc P 2013 DICE 2013R: introduction and User's Manual *Technical Report* (New Haven, CT: Yale University Press)
- O'Gorman P A and Schneider T 2009 The physical basis for increases in precipitation extremes in simulations of XXI-century climate change *Proc. Natl Acad. Sci.* **106** 14773–7
- Park S and Bretherton C S 2009 The university of Washington shallow convection and moist turbulence schemes and their impact on climate simulations with the community atmosphere model *J. Clim.* **22** 3449–69
- Park S, Bretherton C S and Rasch P J 2014 Integrating cloud processes in the community atmosphere model, version 5 *J. Clim.* **27** 6821–56
- Pendergrass A G and Hartmann D L 2014 The atmospheric energy constraint on global-mean precipitation change *J. Clim.* **27** 757–68
- Penner J E, Zhou C and Liu X 2015 Can cirrus cloud seeding be used for geoengineering? *Geophys. Res. Lett.* **42** 8775–82
- Robock A, Oman L and Stenchikov G L 2008 Regional climate responses to geoengineering with tropical and arctic SO<sub>2</sub> injections *J. Geophys. Res.* **113** D16101
- Rogelj J, Luderer G, Pietzcker R C, Kriegler E, Schaeffer M, Krey V and Riahi K 2015 Energy system transformations for limiting end-of-century warming to below 1.5 °C *Nat. Clim. Change* **5** 519–27
- Rotstayn L D and Lohmann U 2002 Tropical rainfall trends and the indirect aerosol effect *J. Clim.* **15** 2103–16
- Sanderson B M, O'Neill B and Tebaldi C 2016 What would it take to achieve the Paris temperature targets? *Geophys. Res. Lett.* **43** 7133–42
- Slingo J M 1987 The development and verification of a cloud prediction scheme for the Ecmwf model *Q. J. R. Meteorol. Soc.* **113** 899–927
- Sourdeval O, Gryspeerd E, Krämer M, Goren T, Delanoë J, Afchine A, Hemmer F and Quaas J 2018 Ice crystal number concentration estimates from lidar-radar satellite remote sensing: I. Method and evaluation *Atmos. Chem. Phys. Discuss.* **18** 14327–50
- Stevens B *et al* 2013 Atmospheric component of the MPI-M earth system model: ECHAM6 *J. Adv. Modeling Earth Syst.* **5** 146–72
- Storelvmo T, Boos W R and Herger N 2014 Cirrus cloud seeding: a climate engineering mechanism with reduced side effects? *Phil. Trans. R. Soc. A* **372** 20140116
- Storelvmo T and Herger N 2014 Cirrus cloud susceptibility to the injection of ice nuclei in the upper troposphere *J. Geophys. Res.: Atmos.* **119** 2375–89
- Storelvmo T, Kristjansson J E, Muri H, Pfeffer M, Barahona D and Nenes A 2013 Cirrus cloud seeding has potential to cool climate *Geophys. Res. Lett.* **40** 178–82
- Sugiyama M, Shiogama H and Emori S 2010 Precipitation extreme changes exceeding moisture content increases in MIROC and IPCC climate models *Proc. Natl Acad. Sci.* **107** 571–5
- Tan I, Storelvmo T and Zelinka M D 2016 Observational constraints on mixed-phase clouds imply higher climate sensitivity *Science* **352** 224–7
- Taylor K E, Stouffer R J and Meehl G 2012 An overview of CMIP5 and the experiment design *Bull. Am. Meteorol. Soc.* **93** 485–98
- Tiedtke M 1989 A comprehensive mass flux scheme for cumulus parameterization in large-scale models *Mon. Weather Rev.* **117** 1179–800
- Tilmes S, Sanderson B M and O'Neill B C 2016 Climate impacts of geoengineering in a delayed mitigation scenario *Geophys. Res. Lett.* **43** 8222–9
- Tilmes S *et al* 2013 The hydrological impact of geoengineering in the geoengineering model intercomparison project (GeoMIP) *J. Geophys. Res.: Atmos.* **118** 11036–58
- van Vuuren D P *et al* 2011 The representative concentration pathways: an overview *Clim. Change* **109** 5–31
- Vaughan N E and Gough C 2016 Expert assessment concludes negative emissions scenarios may not deliver *Environ. Res. Lett.* **11** 095003
- Weitzman M L 2010 What is the 'damages function' for global warming—and what difference might it make? *Clim. Change Econ.* **01** 57–69
- Xia L *et al* 2014 Journal of geophysical research: atmospheres model intercomparison project (GeoMIP) *J. Geophys. Res.: Atmos.* **119** 8695–711
- Zhang G J and McFarlane N A 1995 Sensitivity of climate simulations to the parameterization of cumulus convection in the canadian climate centre general circulation model *Atmosphere—Ocean* **33** 407–46
- Zhang K *et al* 2012 The global aerosol-climate model ECHAM-HAM, version 2: sensitivity to improvements in process representations *Atmos. Chem. Phys.* **12** 8911–49